HHS Public Access

Author manuscript

Nature. Author manuscript; available in PMC 2012 August 02.

Published in final edited form as:

Nature. ; 482(7383): 116–119. doi:10.1038/nature10743.

CYTOCHROME P450 17A1 STRUCTURES WITH PROSTATE CANCER DRUGS ABIRATERONE AND TOK-001

Natasha M. DeVore and **Emily E. Scott**

The Department of Medicinal Chemistry, 1251 Wescoe Hall Dr., The University of Kansas, Lawrence, KS, 66045

Abstract

Cytochrome P450 17A1 (P450c17) catalyzes the biosynthesis of androgens in humans[1]. Since prostate cancer cells proliferate in response to androgen steroids[2,3], CYP17A1 inhibition is a new strategy to prevent androgen synthesis and treat lethal metastatic castration-resistant prostate cancer[4], but drug development has been hampered by the lack of a CYP17A1 structure. Here we report the only known structures of CYP17A1, which contain either abiraterone, a first-in-class steroidal inhibitor recently approved by the FDA for late-stage prostate cancer[5], or TOK-001, another inhibitor in clinical trials[4,6]. Both bind the heme iron forming a 60° angle above the heme plane, packing against the central I helix with the 3β-OH interacting with N202 in the F helix. Importantly, this binding mode differs substantially from those predicted by homology models or from steroids in other cytochrome P450 enzymes with known structures, with some features more similar to steroid receptors. While the overall CYP17A1 structure provides a rationale for understanding many mutations found in patients with steroidogenic diseases, the active site reveals multiple steric and hydrogen bonding features that will facilitate better understanding of the enzyme's dual hydroxylase and lyase catalytic capabilities and assist in rational drug design. Specifically, structure-based design is expected to aid development of inhibitors that bind only CYP17A1 and solely inhibit its androgen-generating lyase activity to improve treatment of prostate and other hormone-responsive cancers.

Cytochrome P450 17A1 (CYP17A1, P450c17, EC 1.14.99.9) is a membrane-bound dual-function monooxygenase with a critical role in the synthesis of many human steroid hormones[1]. CYP17A1 17α-hydroxylase activity is required for generation of glucocorticoids like cortisol, while its hydroxylase and 17,20-lyase activities are required for production of androgenic and estrogenic sex steroids (fig S1). CYP17A1 is an important

---

Correspondence and requests for materials should be addressed to EES (eescott@ku.edu).

Supplemental Information is linked to the online version of the paper at www.nature.com/nature.

Author Contributions ND engineered, expressed, characterized, purified, and crystallized CYP17A1 under the direction of EES. ND and EES jointly performed X-ray diffraction experiments, solved and refined the structures, and wrote the manuscript. ND performed the docking studies of CYP17A1.

Author Information Atomic coordinates and structure factors for the reported crystal structures have been deposited with the Protein Data Bank under the accession codes 3RUK for CYP17A1 with abiraterone and 3SWZ for CYP17A1 with TOK-001.

The authors declare no competing financial interests.

target for the treatment of breast and prostate cancers that proliferate in response to estrogens and androgens[2,3]. In the absence of structural information, CYP17A1 inhibitors have been designed that are thought to bind the cytochrome P450 heme iron[4], but it has been difficult to rationalize or predict other structural features critical for effective, selective CYP17A1 inhibition. In addition, structural information is important to understand 17α-hydroxylase deficiencies and potentially polycystic ovary disease[7]. We determined structures of human CYP17A1 bound to two clinically-relevant CYP17A1 inhibitors (fig. S2). Abiraterone is the active form of a prodrug recently approved by the FDA for metastatic prostate cancer[5,8] and under investigation for breast cancer[9]. TOK-001 is currently in clinical trials for prostate cancer[4].

A truncated, His-tagged version of the human CYP17A1 protein was generated from a synthetic cDNA engineered to remove the single N-terminal transmembrane helix and expressed in *E. coli*. Resulting CYP17A1 was membrane-bound, so was solubilized with detergent before purification. This CYP17A1 binds abiraterone (fig. 1a) and TOK-001 (not shown) with absorbance decreases at 402 nm and increases at 424 nm, consistent with nitrogen binding to the heme iron (type II interaction) with K_d values of <100 nM (fig. 1a inset). Similar titrations with substrates progesterone (fig. 1b) and pregnenolone (not shown) revealed absorbance decreases at 419 nm and increases at 385 nm, indicative of ligand displacing water from the heme (type I interaction). CYP17A1 binds pregnenolone (K_d <100 nM, not shown) significantly more tightly than progesterone (K_d 229±14 nM; fig. 1b inset). In our hands, full-length enzyme[10] had a similar k_{cat} and 3-fold higher K_m (k_{cat} 1.31±0.03 min^{-1}, K_m 11.4±0.7 μM) compared to the truncated form (k_{cat} 1.31±0.03 min^{-1}, K_m 3.7±0.3 μM). IC_{50} values for abiraterone (201±1 nM) were lower than for TOK-001 (503.0±1.0 nM) (fig. 1c). Thus, truncated human CYP17A1 is a functional enzyme in terms of ligand binding, catalytic function, and inhibition.

Both structures with abiraterone (2.6 Å) and TOK-001 (2.4 Å) demonstrate the characteristic cytochrome P450 fold (fig. 2a) and have four very similar protein copies in each asymmetric unit (Table S1). Consistent with spectral binding data, abiraterone and TOK-001 bind with the nitrogen of the C17 pyridine or benzimidazole, respectively, forming a coordinate covalent bond with heme iron (fig. 2b and 2d). The steroid nucleus of these inhibitors rise at a 60° angle above the heme plane, directed between the F and G helices (fig. 2b and 2d), and essentially overlap (fig. 2f). The unsubstituted α face packs flat against the I helix where G301, A302, and adjacent residues form a highly complementary hydrophobic planar surface (fig. 2b). The 3β-OH groups of abiraterone (fig. 2b) and TOK-001 (fig. 2d) hydrogen bond with N202 in the F helix (~2.6 Å and ~2.4 Å, respectively).

Although inhibitors occupy the majority of the enclosed active site, the void extends beyond these ligands in several directions. First, the active site wall nearest the inhibitor β face is not as complementary to the steroid nucleus as for the α face. The C18 and C19 methyl groups project toward a crevice between the B′ helix, the β4 loop, and the loop following the F helix (fig. 2b). Only three side chains of the cavity wall come within 4 Å of C18 or C19. The cavity wall facing the β face of abiraterone or TOK-001 is primarily lined with hydrophobic atoms of A105, S106, A113, F114, I206, L209, V236, and V482 (fig. 2c), but there are two notable exceptions. R239 and D298 extend from the G and I helices, respectively, to orient

their basic and acidic termini toward C6. These two polar side chains flank a substantial extension of the active site void adjacent C6. Second, in the abiraterone structure there is additional volume available adjacent to the pyridine ring bordered by V366, A367, I371, and V483 (fig. 2c), which is occupied by benzimidazole in the TOK-001 structure (fig. 2e). Finally, the most substantial active site cavity extension is from the 3β-OH of the inhibitors over the top of helix I and along the underside of helices F and G. This cavity is mostly lined by hydrophobic residues (I198, L243, F300), but its “roof” is bordered by several polar F and G helix residues (Y201, N202, R239, fig. 2c) that interact with, or are located near, waters in this region. The cavity containing TOK-001 is similar but slightly smaller over helix I (fig. 2e).

The single direct hydrogen bond between inhibitors and the protein is part of a larger hydrogen bonding network. In the abiraterone complex this network involves N202, E305, several conserved water molecules, R239, the backbone carbonyl of G297, and in some molecules Y201 (fig. 3). While Y201 is not within hydrogen bonding distance to these waters for molecules A and B, the side chain rotates slightly toward abiraterone in molecules C and D to interact with one or both of the water molecules. TOK-001 has a very similar hydrogen bonding network (fig S3). These interactions are strongly reminiscent of those conserved in the androgen, estrogen, glucocorticoid, mineralocorticoid, and progesterone receptors[11] (fig. 4a,b). In each receptor, the 3β-OH or 3-keto of steroids binds within a deep receptor pocket and forms hydrogen bonds with an arginine, a glutamine/glutamate, and often a conserved water molecule. These interactions are critical for ligand recognition by hormone receptors[12] and may also contribute to CYP17A1 selectivity for pregnenolone, progesterone, and their 17α-hydroxy derivatives. Notably, TOK-001 is both a CYP17A1 inhibitor and androgen receptor antagonist[13] and the similarity of these binding modes is likely the reason for this dual mechanism of action.

Orientations of the native CYP17A1 substrates are of substantial value in understanding the function of this enzyme. Pregnenolone and progesterone were docked into the CYP17A1/abiraterone structure modeled as the Fe(IV)=O (compound I) catalytic state. Progesterone maintained the N202 hydrogen bond. The distances from C17 and C16 to the catalytic oxygen were 3.7 Å and 3.9 Å, respectively, consistent with the observed 17α-OH (major) and 16α-OH (minor) progesterone metabolites. The pregnenolone C17 atom was 3.6 Å from the compound I oxygen and the 3β-OH hydrogen bonded to N202 (Fig S4). However, the active site topology may be altered in the presence of substrates and this is an important area for further investigation.

CYP17A1 can be compared to three other P450 enzymes involved in steroidogenesis or cholesterol metabolism with reported steroid complex structures: CYP19A1 (aromatase)[14]; CYP11A1 (cholesterol side-chain cleavage enzyme)[15]; and CYP46A1, a cholesterol 24-hydroxylase[16]. Although all four enzymes maintain the canonical cytochrome P450 fold, the other three orient steroids in the opposite direction from CYP17A1. All three have the steroid ligand positioned over the K-L loop directed towards theβ1 sheet as in CYP11A1 (fig. 4c), instead of oriented toward helices F and G.

Over 50 CYP17A1 mutations have been identified, most in patients with 17-hydroxylase deficiencies. The biochemical effects of many clinical mutations can be rationalized by examining the CYP17A1 structure (Fig S5, Table S2). Mutations R96W, R125Q, H373D/N, and R440H/C all alter residues that directly interact with the heme propionates and likely disrupt heme binding, consistent with complete loss of activity[17–22]. Mutations E305G, R347H/C, R358Q, and R449A eliminate only the lyase activity of CYP17A1[23–25]. E305 hydrogen bonds to N202 in the active site, suggesting a role in substrate positioning, while the other residues are on the proximal face of the protein (fig. S5), consistent with their proposed role in cytochrome b_5 binding[23,26], which promotes lyase activity. Finally, reduction of the minor 16α-hydroxyprogesterone metabolite is reported for the artificial mutation A105L[27], consistent with its location in the active site facing the β face where the additional bulk may reduce the steroid movement within the active site.

Abiraterone and TOK-001 have several features which make them effective inhibitors of CYP17A1: 1) a heterocyclic nitrogen that coordinates to the heme iron, 2) a planar α face to pack against the I helix, and 3) hydrogen bonding interactions of 3β-OH with conserved polar residues in a hydrogen binding network. These structures provide a model for the binding of substrates and other inhibitors that is very different from binding orientations previously proposed by homology modeling and docking studies and from those demonstrated in other steroid-metabolizing cytochrome P450 enzymes. Perhaps most importantly, the cavity observed is not bilobed as predicted by many modeling studies[28,29]. CYP17A1 interactions with these inhibitors are instead more reminiscent of steroid binding to steroid receptors, which may be the genesis of the TOK-001 dual mechanism of action. Thus, these structures contribute to a better understanding of the function and inhibition of CYP17A1 in a way that should substantially benefit the understanding of enzyme dysfunction in clinical disease and enable structure-based drug design of CYP17A1 inhibitors for treating hormone-responsive cancers, especially prostate cancer.

Methods Summary

A synthetic cDNA for human CYP17A1 was modified to delete residues 2–19, substitute the hydrophilic sequence ^{20}RRCP^{23} with ^{20}AKKT^{23}, and add a C-terminal four histidine tag (fig. S6) before cloning into the **pCWori^{+}** plasmid and overexpression in *E. coli* JM109 cells. Protein was purified by nickel affinity, cation exchange, and size exclusion chromatography. Abiraterone was synthesized (Methods). Binding affinities were determined using a UV/vis spectral shift assay. Progesterone 17α-hydroxylation was evaluated using HPLC separation and UV detection. For crystallography, inhibitors were included throughout purification. Crystals were grown from CYP17A1 (30 mg/mL) complexed with inhibitor using hanging-drop vapor diffusion to equilibrate against 30% PEG 3350, 0.175 M Tris, pH 8.5, 0.30 M ammonium sulfate, and 3% glycerol. Diffraction data was collected and phased by molecular replacement. Iterative model building and refinement generated the final model. Substrates were docked using Surflex-Dock[30].

Methods

Synthesis and characterization of abiraterone, 17-(3-pyridyl)androsta-5,16-dien-3β-ol

A stirred solution of 17-iodoandrosta-5,16-dien-3β-ol (600 mg, 1.5 mmol) in THF (20mL) in a 100 mL round-bottomed flask was purged with argon. Bis(triphenylphosphine) palladium (II) chloride catalyst (11 mg, 0.016 mmol) was added, followed by diethyl(3-pyridyl)borane (265 mg, 1.8 mmol). To the resultant orange solution, an aqueous solution of sodium carbonate (2M, 5 mL) was added. The flask was fitted with a reflux condenser and the apparatus purged again with argon. The mixture was then heated under reflux (~80 °C) with stirring for 4 days then allowed to cool. The mixture was poured into water and extracted with hot toluene (3x30 mL). The toluene extracts were dried (Na_2CO_3) and concentrated. Column chromatography was performed with Et_2O/toluene (1:2) as the eluent to give abiraterone (350 mg, 66%) as a white crystalline solid: mp 228–230 °C; IR ν_{max} 3307 cm^{-1} (OH str); ^1H NMR δ 1.07 (s, 3, H-19), 1,09 (s, 3, H-18), 3.54 (m, 1, H-3α), 5,41 (dm, 1, J = 5.2 Hz, H-6), 6.01 (m, 1, H-16), 7.24 (dd, 1, pyridyl H-5), 7.66 (dd, 1, pyridyl H-4), 8.47 (dd, 1, pyridyl H-6), 8.63 (d, 1, pyridyl H-2); ^{13}C NMR δ 151.69, 147.92, 147.84, 141.19, 133.68, 132.98, 129.24, 123.03, 121.32, 71.65, 57.56, 50.36, 47.34, 42.32, 37.19, 36.71, 35.26, 31.81, 31.64, 30.45, 20.88, 19.35, 16.59. The HRMS calculated m/z $C_{24}H_{32}NO$ $[M+H]^+$ is 350.2484. The experimental value was 350.2491. Abiraterone was 99% pure by LCMS.

CYP17A1 design, expression, and purification

The human CYP17A1 cDNA was synthesized with codon optimization for *E. coli* expression (Blue Heron Biotechnology, Bothell, WA). A truncated and His-tagged construct was generated by truncation of the N-terminal transmembrane helix (Δ2–19), substitution of ^{20}RRCP^{23} with ^{20}AKKT^{23}, and addition of a C-terminal four-residue histidine tag (fig. S6). N-terminal modifications were designed to increase solubility. This altered cDNA was inserted into the **pCWori$^+$** expression vector and expressed in *E. coli* JM109 cells.

Cells were grown, harvested, and disrupted as described[10,31]. After centrifugation (5000 × g), CYP17A1 was solubilized with either 4.8 mM Cymal-5 (for crystallography; Affymetrix, Santa Clara, CA) or 2% Emulgen 913 (for assays; Desert Biologicals, Phoenix, AZ), followed by ultracentrifugation (80,000 × g) for 60 minutes. The lysate was loaded onto a NTA-agarose (Qiagen, Valencia, CA) column and purified as reported[31]. Eluted CYP17A1 fractions were pooled, diluted 5-fold with CM buffer (50mM Tris, pH 7.4, 20% glycerol, 100 mM glycine, 1 mM EDTA), and loaded on a HiTrap CM fast flow column (GE Healthcare, Uppsala, Sweden). Protein was eluted in CM buffer with 0.5 M NaCl, concentrated to ~1 mL, and loaded on a Superdex 200 16/60 size exclusion column (GE Healthcare). For crystallography 10 μM abiraterone or TOK-001 (Shanghai Haoyuan Chemexpress Co., Shanghai, China) was added to all buffers.

Protein crystallization, data collection, and structure determination

CYP17A1 crystals were grown using hanging drop vapor diffusion equilibration. CYP17A1 (30 mg/mL) in CM buffer supplemented with 10 μM abiraterone or TOK-001, 2.4 mM Cymal-5, and 0.5 M NaCl was equilibrated against 30% PEG 3350, 0.175 M Tris, pH 8.5,

0.30 M ammonium sulfate, and 3% glycerol at 20 C. Crystals were cryoprotected in 7:1 mother liquor:ethylene glycol and flash cooled in liquid nitrogen. Native data sets were collected at 0.98 Å, 100 K at the Stanford Synchrotron Radiation Laboratory beamline 9–2. Data were processed using Mosflm[32] and Scala[33]. The abiraterone complex was solved by molecular replacement using BALBES[34] with a final search model based on CYP2R1 (PDB 3CZH) and the TOK-001 structure solved using Phaser[33] with the abiraterone structure as a search model. Model building and refinement were accomplished iteratively using COOT[35] and Refmac5[36] in CCP4[33]. Structure validation was performed using WHATCHECK[37] and PROCHECK[38]. Ramachandran plot analysis reveals percent favorable/additional allowed/ generously allowed/disallowed residues are 86.3/13.2/0.5/0.0 (abiraterone structure) and 86.2/13.3/0.5/0.0 (TOK-001 structure). X-ray statistics are provided (Table S1). Probe-occupied voids were calculated using VOIDOO[40] (probe radius=1.4 Å; grid mesh=0.4 Å). All figures were prepared using MacPyMOL[39].

Docking

The CYP17A1 active site was defined as described for other cytochromes P450[40] with the addition of an oxygen molecule directly coordinated to the heme to mimic Compound I of the cytochrome P450 catalytic cycle. Substrate coordinates were prepared and energy minimized with SYBYL (Tripos, St. Louis, MO). Charges were assigned using the Gasteiger and Marsili method. Surflex-Dock (Tripos International, St. Louis, Missouri) was used to dock ligands as previously described[40]. The active site was a 10 Å sphere around the heme and pregnenolone. Movement of pregnenolone within the active site was not substantial with the distance of C17 to O=Fe(IV) 4.5 Å, C16 to O=Fe(IV) of 4.5 Å, and a distance from C21 to O=Fe(IV) of 3.0 Å for the lowest energy pose.

Enzyme activity and IC_{50} determinations

Progesterone 17α-hydroxylation was evaluated using a modified HPLC method with UV-detection[41]. CYP17A1 (50 pmol) and rat NADPH-cytochrome P450 reductase[42] 1:4 were mixed, incubated on ice (20 minutes), and added to buffer (50 mM Tris, pH 7.4 and 5 mM $MgCl_2$) containing progesterone (0 – 50 μM) to a total volume of 500 μL. Phosphatidylcholine (25 μg) was included for side-by-side kinetic comparisons with the full-length enzyme[10]. For IC_{50} determinations, inhibitors concentrations were 0–1500 nM for abiraterone and 0–3000 nM for TOK-001. After warming (37° C, 3 minutes), reactions were initiated by NADPH addition (20 μL 25 mM), incubated for 10 minutes (37° C), and quenched with 20% trichloroacetic acid (300 μL) and placed on ice. The 17α-hydroxyprogesterone metabolite was identified by UV detection at 248 nm following HPLC separation and coeluted with authentic standards. The HPLC mobile phase was 40% acetonitrile, 60% water with 1% acetic acid and run at 1 mL/min (Phenomenex, Luna 5 μ, C18, 50 × 4.6 mm).

Ligand binding assays

Ligand binding assays based on spectral differences detected upon ligand titration were performed essentially as described[40] except that the CYP17A1 concentration was 0.1 μM, the path length was 5 cm, and the tight binding equation was used.

Functional data was analyzed using Prism (GraphPad Software, La Jolla, CA) and presented as mean ± standard error.

Supplementary Material

Refer to Web version on PubMed Central for supplementary material.

Acknowledgments

X-ray data was collected at the Stanford Synchrotron Radiation Lightsource, a national user facility operated by Stanford University on behalf of the U.S. Department of Energy, Office of Basic Energy Sciences. The SSRL Structural Molecular Biology Program is supported by the DOE Office of Biological and Environmental Research, and by the National Institutes of Health, National Center for Research Resources, Biomedical Technology Program, and the National Institute of General Medical Sciences. We thank Chun-Jing Liu and the KU COBRE Center for Cancer Experimental Therapeutics for synthesizing abiraterone (NIH RR030926), Michael R. Waterman for the full-length CYP17A1 construct, Jenna Wang for assistance with the Fe(IV)=O construct used in docking, and Andi Skinner and Jeff Aube for manuscript suggestions. This research was funded by the National Institutes of Health via the KU COBRE Center for Protein Structure and Function (NIH RR17708) and GM076343.

References

1. Miller WL, Auchus RJ. The molecular biology, biochemistry, and physiology of human steroidogenesis and its disorders. Endocr Rev. 2011; 32:81–151. [PubMed: 21051590]
2. Attard G, Reid AH, Olmos D, de Bono JS. Antitumor activity with CYP17 blockade indicates that castration-resistant prostate cancer frequently remains hormone driven. Cancer Res. 2009; 69:4937–4940. [PubMed: 19509232]
3. Yap TA, Carden CP, Attard G, de Bono JS. Targeting CYP17: Established and novel approaches in prostate cancer. Curr Opin Pharmacol. 2008; 8:449–457. [PubMed: 18619560]
4. Vasaitis TS, Bruno RD, Njar VC. CYP17 inhibitors for prostate cancer therapy. J Steroid Biochem Mol Biol. 2011; 125:23–31. [PubMed: 21092758]
5. de Bono JS, et al. Abiraterone and increased survival in metastatic prostate cancer. N Engl J Med. 2011; 364:1995–2005. [PubMed: 21612468]
6. Molina A, Belidegrun A. Novel therapeutic strategies for castration resistant prostate cancer: Inhibition of persistent androgen production and androgen receptor mediated signaling. J Urol. 2011; 185:787–794. [PubMed: 21239012]
7. Auchus RJ, Geller DH, Lee TC, Miller WL. The regulation of human P450c17 activity: Relationship to premature adrenarche, insulin resistance and the polycystic ovary syndrome. Trends Endocrinol Metab. 1998; 9:47–50. [PubMed: 18406239]
8. Attard G, et al. Phase I clinical trial of a selective inhibitor of CYP17, abiraterone acetate, confirms that castration-resistant prostate cancer commonly remains hormone driven. J Clin Oncol. 2008; 26:4563–4571. [PubMed: 18645193]
9. Brode A, Njar V, Macedo LF, Vasitis TS, Sabnis G. The Coffey Lecture: Steroidogenic enzyme inhibitors and hormone dependent cancer. Urol Oncol. 2009; 27:53–63. [PubMed: 19111799]
10. Imai T, et al. Expression and purification of functional human 17α-hydroxylase/17,20-lyase (P450c17) in *Escherichia coli*. Use of this system for study of a novel form of combined 17α-hydroxylase/17,20-lyase deficiency. J Biol Chem. 1993; 268:19681–19689. [PubMed: 8396144]
11. Huang P, Chandra V, Rastinejad F. Structural overview of the nuclear receptor superfamily: Insights into physiology and therapeutics. Annu Rev Physiol. 2009; 72:247–272. [PubMed: 20148675]
12. Pereira de Jesus-Tran K, et al. Comparison of crystal structures of human androgen receptor ligand-binding domain complexed with various agonists reveals molecular determinants responsible for binding affinity. Protein Sci. 2006; 15:987–999. [PubMed: 16641486]
13. Vasaitis T, et al. Androgen receptor inactivation contributes to antitumor efficacy of 17α-hydroxylase/17,20-lyase inhibitor 3β-hydroxy-17-(1H-benzimidazole-1-yl)androsta-5,16-diene in prostate cancer. Mol Cancer Ther. 2008; 7:2348–2357. [PubMed: 18723482]

14. Ghosh D, Griswold J, Erman M, Pangborn W. Structural basis for androgen specificity and oestrogen synthesis in human aromatase. Nature. 2009; 457:219. [PubMed: 19129847]
15. Mast N, et al. Structural basis for three-step sequential catalysis by the cholesterol side chain cleavage enzyme CYP11A1. J Biol Chem. 2011; 7:5607. [PubMed: 21159775]
16. Mast N, et al. Crystal structures of substrate-bound and substrate-free cytochrome P450 46A1, the principal cholesterol hydroxylase in the brain. Proc Natl Acad Sci USA. 2008; 105:9546–9551. [PubMed: 18621681]
17. Dhir V, et al. Steroid 17α-hydroxylase deficiency: Functional characterization of four mutations (A174E, V178D, R440C, L465P) in the CYP17A1 gene. J Clin Endocrinol Metab. 2009; 94:3058–3064. [PubMed: 19454579]
18. Rosa S, et al. Clinical, genetic and functional characteristics of three novel CYP17A1 mutations causing combined 17α-hydroxylase/17,20-lyase deficiency. Horm Res Paediatr. 2009; 73:198–204. [PubMed: 20197673]
19. Katsumata N, Ogawa E, Fujiwara I, Fujikura K. Novel CYP17A1 mutation in a Japanese patient with combined 17α-hydroxylase/17,20-lyase deficiency. Metabolism. 2010; 59:275–278. [PubMed: 19793597]
20. Ergun-Longmire B, et al. Two novel mutations found in a patient with 17α-hydroxylase enzyme deficiency. J Clin Endocrinol Metab. 2006; 91:4179–4182. [PubMed: 16849412]
21. Sahakitrungruang T, Tee MK, Speiser PW, Miller WL. Novel P450c17 mutation H373D causing combined 17α-hydroxylase/17,20-lyase deficiency. J Clin Endocrinol Metab. 2009; 94:3089–3092. [PubMed: 19470621]
22. Biason-Lauber A, et al. 17α-hydroxylase/17,20-lyase deficiency as a model to study enzymatic activity regulation: Role of phosphorylation. J Clin Endocrinol Metab. 2000; 85:1226–1231. [PubMed: 10720067]
23. Lee-Robichaud P, et al. The cationic charges on Arg347, Arg358 and Arg449 of human cytochrome P450c17 (CYP17) are essential for the enzyme's cytochrome b_5-dependent acyl-carbon cleavage activities. J Steroid Biochem Mol Biol. 2004; 92:119–130. [PubMed: 15555906]
24. Gupta MK, Geller DH, Auchus RJ. Pitfalls in characterizing P450c17 mutations associated with isolated 17,20-lyase deficiency. J Clin Endocrinol Metab. 2001; 86:4416–4423. [PubMed: 11549685]
25. Tiosano D, et al. Metabolic evidence for impaired 17α-hydroxylase activity in a kindred bearing the E305G mutation for isolate 17,20-lyase activity. Eur J Endocrinol. 2008; 158:385–392. [PubMed: 18299473]
26. Auchus RJ, Lee TC, Miller WL. Cytochrome b_5 augments the 17,20-lyase activity of human P450c17 without direct electron transfer. J Biol Chem. 1998; 273:3158–3165. [PubMed: 9452426]
27. Swart AC, Storbeck KH, Swart P. A single amino acid residue, Ala 105, confers 16α-hydroxylase activity to human cytochrome P450 17α-hydroxylase/17,20 lyase. J Steroid Biochem Mol Biol. 2010; 119:112. [PubMed: 20043997]
28. Haider SM, Patel JS, Poojari CS, Neidle S. Molecular modeling on inhibitor complexes and active-site dynamics of cytochrome P450 C17, a target for prostate cancer therapy. J Mol Biol. 2010; 400:1078–1098. [PubMed: 20595043]
29. Jagusch C, et al. Synthesis, biological evaluation and molecular modelling studies of methyleneimidazole substituted biaryls as inhibitors of human 17α-hydroxylase-17,20-lyase (CYP17). Part I: Heterocyclic modifications of the core structure. Bioorg Med Chem. 2008; 16:1992–2010. [PubMed: 18061460]
30. Jain AN. Surflex: fully automatic flexible molecular docking using a molecular similarity-based search engine. J Med Chem. 2003; 46:499–511. [PubMed: 12570372]
31. Pechurskaya TA, Lukashevich OP, Gilep AA, Usanov SA. Engineering, expression, and purification of "soluble" human cytochrome P45017α and its functional characterization. Biochemistry (Mosc). 2008; 73:806–811. [PubMed: 18707589]
32. Leslie, AGW. MOSFLM 60. Cambridge, UK: 1998.
33. Evans P. The CCP4 suite: Programs for protein crystallography. Acta Crystallogr D. 1994; 50:760–763. [PubMed: 15299374]

34. Long F, Vagin AA, Young P, Murshudov GN. BALBES: A Molecular Replacement Pipeline. Acta Crystallogr D. 2008; 64:125–132. [PubMed: 18094476]

35. Emsley P, Cowtan K. Coot: Model-building tools for molecular graphics. Acta Crystallogr D. 2004; 60:2126–2132. [PubMed: 15572765]

36. Murshudov GN, Vagin AA, Dodson EJ. Refinement of macromolecular structures by the maximum-likelihood method. Acta Crystallogr D. 1996; 53:240–255. [PubMed: 15299926]

37. Hooft RW, Vriend G, Sander C, Abola EE. Errors in protein structures. Nature. 1996; 381:272–272. [PubMed: 8692262]

38. Laskowski RA, MacArthur MW, Moss DS, Thornton JM. PROCHECK - a program to check the stereochemical quality of protein structures. J App Cryst. 1993; 26:283–291.

39. Schrodinger, LLC. 2010

40. DeVore NM, et al. Key residues controlling binding of diverse ligands to human cytochrome P450 2A enzymes. Drug Metab Dispos. 2009; 37:1319–1327. [PubMed: 19251817]

41. Hutschenreuter TU, Ehmer PB, Hartmann RW. Synthesis of hydroxy derivatives of highly potent non-steroidal CYP 17 inhibitors as potential metabolites and evaluation of their activity by a non cellular assay using recombinant human enzyme. J Enzyme Inhib Med Chem. 2004; 19:17–32. [PubMed: 15202489]

42. Shen AL, Porter TD, Wilson TE, Kasper CB. Structural analysis of the FMN binding domain of NADPH-cytochrome P-450 oxidoreductase by site-directed mutagenesis. J Biol Chem. 1989; 264:7584–7589. [PubMed: 2708380]

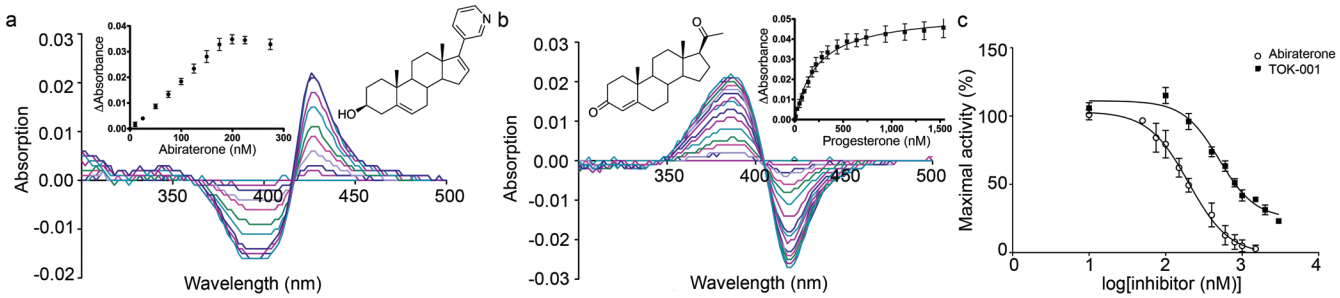

Figure 1. Function of CYP17A1 and inhibition by clinical compounds

a, CYP17A1 titration with abiraterone (10–274 nM) yields progressive shifts in the UV/Vis difference spectrum typical of nitrogen binding to heme iron. b, Similar titration with progesterone (10–1535 nM) indicates water displacement from the heme iron. c, IC_{50} of abiraterone (circles) and TOK-001 (squares) for progesterone 17 α–hydroxylation.

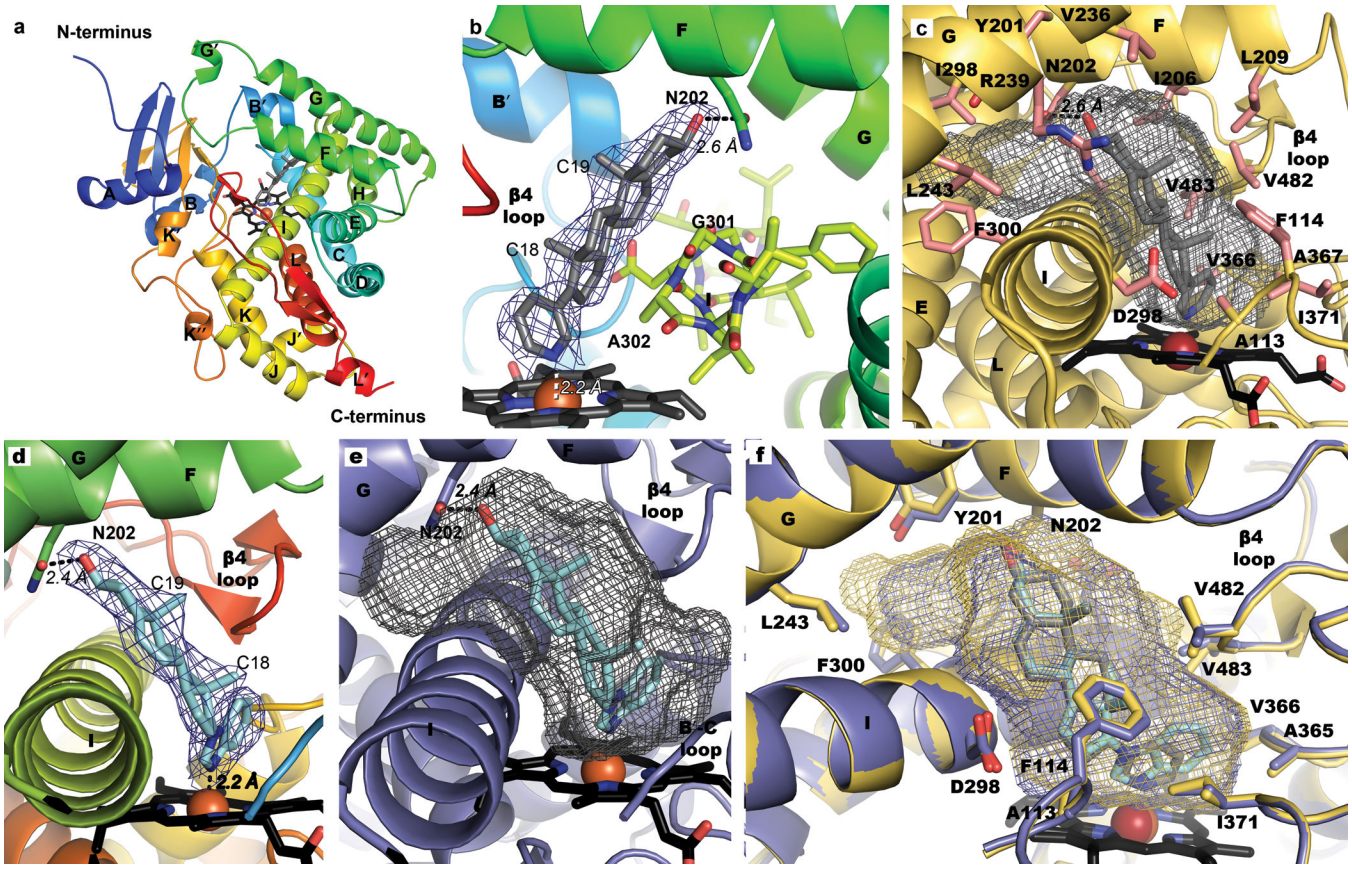

Figure 2. CYP17A1 ligand binding

Stick and sphere representations have non-carbon atoms indicated as: blue, N; red, O; rust, Fe; heme, black; abiraterone, grey; TOK-001, cyan. a, CYP17A1/abiraterone structure colored from N-terminus (blue) to C-terminus (red). b, Abiraterone binds (2|Fo|−|Fc| density at 1 σ, blue mesh) at ~60° from heme against helix I (yellow). c, Abiraterone cavity (grey mesh), ~180° rotation from 2b. d, TOK-001 binding (2|Fo|−|Fc| density at 1 σ, blue mesh). e, TOK-001 cavity (grey mesh). f, Overlay of abiraterone (yellow) and TOK-001 (purple) structures with respective voids (mesh). B′ helix removed from panels c-f to view ligands.

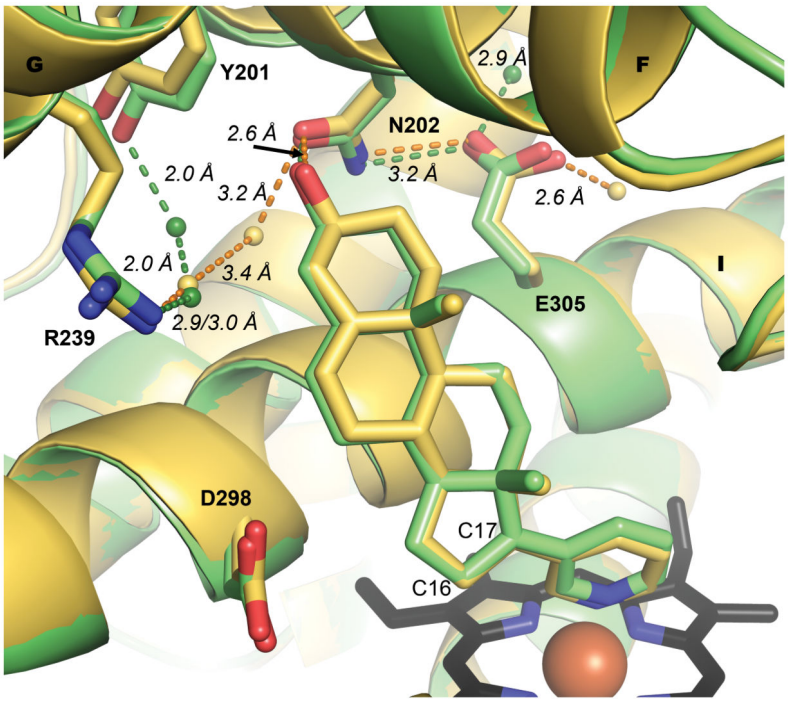

Figure 3. Hydrogen bond network with abiraterone

CYP17A1 has a hydrogen bonding network at the top of the active site that interacts with abiraterone. Molecule A/B (yellow) and C/D (green) have slightly different networks with the main difference being the involvement of Y201. Water molecules are indicated by small spheres. C17 and C16 are labeled. Hydrogen bonds indicated by dashed lines with distances indicated.

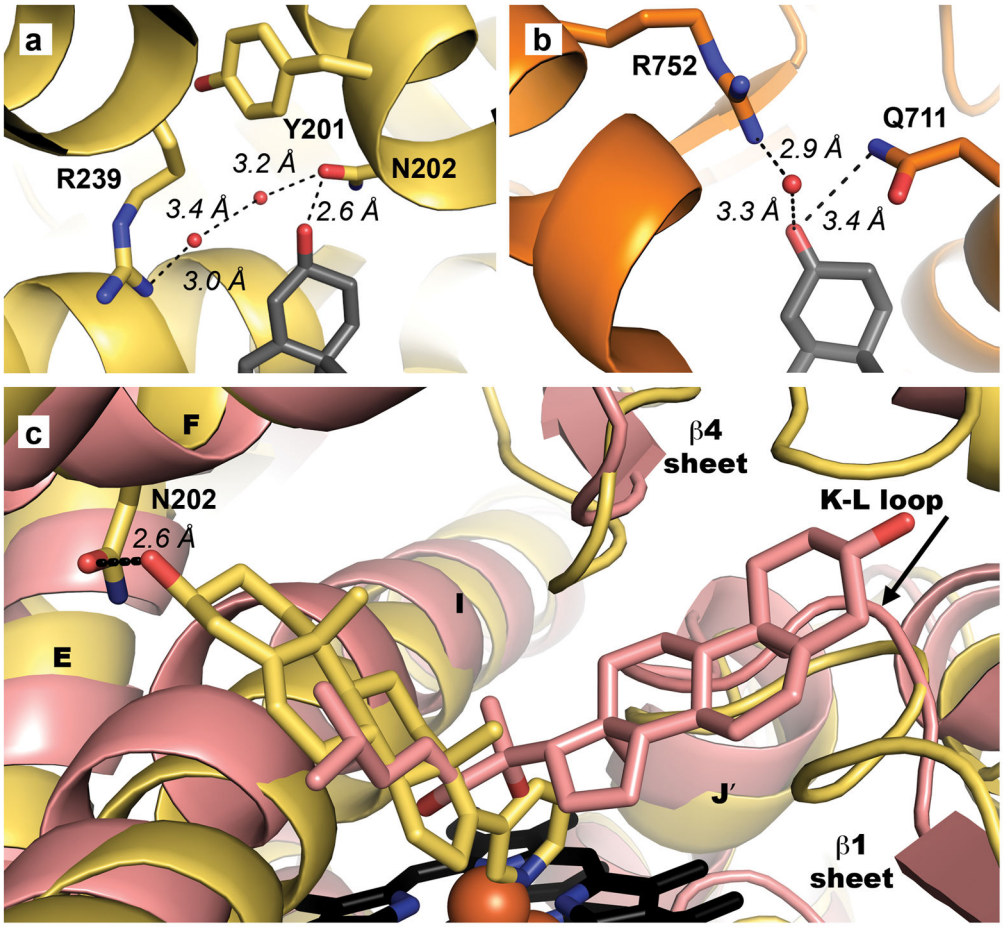

Figure 4. CYP17A1 compared to the androgen receptor and CYP11A1

a, The hydrogen bonding network near the abiraterone 3β-OH involves N202, R239, and conserved waters. b, The androgen receptor (PDB 3L3X) has a similar hydrogen bond network with R752, Q711, and several waters interacting with the dihydrotestosterone ketone. c, Overlay of CYP17A1 with abiraterone (yellow) and CYP11A1 with 20,22-dihydroxycholesterol (PDB 3NA0, pink) shows dramatically different steroid orientations.